



delli Carri, A., Weekes, B., Di Maio, D., & Ewins, D. J. (2017).  
Extending modal testing technology for model validation of  
engineering structures with sparse nonlinearities: A first case study.  
*Mechanical Systems and Signal Processing*, 84 Part B, 97-115.  
<https://doi.org/10.1016/j.ymssp.2016.04.012>

Peer reviewed version

License (if available):  
CC BY-NC-ND

Link to published version (if available):  
[10.1016/j.ymssp.2016.04.012](https://doi.org/10.1016/j.ymssp.2016.04.012)

[Link to publication record on the Bristol Research Portal](#)  
PDF-document

This is the author accepted manuscript (AAM). The final published version (version of record) is available online via Elsevier at <http://dx.doi.org/10.1016/j.ymssp.2016.04.012>.

## University of Bristol – Bristol Research Portal

### General rights

This document is made available in accordance with publisher policies. Please cite only the published version using the reference above. Full terms of use are available:  
<http://www.bristol.ac.uk/red/research-policy/pure/user-guides/brp-terms/>

## **Extending Modal Testing Technology for Model Validation of Engineering Structures with Sparse Nonlinearities: A First Case Study.**

by

A delli Carri\*, B Weekes, D Di Maio, D J Ewins

### **ABSTRACT**

Modal testing is widely used today as a means of validating theoretical (Finite Element) models for the dynamic analysis of engineering structures, prior to these models being used for optimisation of product design. Current model validation methodology is confined to linear models and is primarily concerned with (i) correcting inaccurate model parameters and (ii) ensuring that sufficient elements are included for these cases, using measured data. Basic experience is that this works quite well, largely because the weaknesses in the models are relatively sparse and, as a result, are usually identifiable and correctable. The current state-of-the-art in linear model validation has contributed to an awareness that residual errors in FE models are increasingly the consequence of some unrepresented nonlinearity in the structure. In these cases, additional, higher order *parameters* are required to improve the model so that it can represent the nonlinear behaviour. This is opposed to the current practice of simply refining the mesh. Again, these nonlinear features are generally localised, and are often associated with joints. We seek to provide a procedure for extending existing modal testing to enable these nonlinear elements to be addressed using current nonlinear identification methods directed at detection, characterisation, location and then quantification - in order to enhance the elements in an FE model as necessary to describe nonlinear dynamic behaviour. Emphasis is placed on the outcome of these extended methods to relate specifically to the physical behaviour of the relevant components of the structure, rather than to the nonlinear response characteristics that are the result of their presence.

**Key Words:** modal testing; nonlinear structures; model upgrading; model updating; model validation

\*[a.dellicarri@bristol.ac.uk](mailto:a.dellicarri@bristol.ac.uk) - +447873191850

# 1 Introduction

## 1.1 Background

In recent years, there has been a growing interest in the significant prospect of extending the updating of structural dynamics models for the design of critical structures so as to make them valid for the higher levels of excitation and response that are encountered under service conditions, as opposed to those usually used in laboratory tests. This development frequently involves the inclusion of nonlinear behaviour and the transition from linear to nonlinear characterisation of complex engineering structures is a daunting prospect. However, it is considered probable that many practical cases will have the possibility of significant improvement to the relevant models for a relatively modest extension of linear model validation procedures. Essentially, the nonlinear features in many structures and machines tend to be localised, and even sparse, and so by focussing on the most significant of the nonlinear regions of the structure, it is likely that a notable improvement over the underlying linear representation can be gained without a fundamental re-think of the whole model.

A methodology for such an extension to the modal testing that is undertaken for traditional linear model validation has recently been proposed and described in [1]. One constraint on this new procedure is that it should require the minimum of additional test equipment, practice and analysis software beyond that routinely available in today's high-technology industries. Ref [1] includes mention of a range of algorithms that are currently available or under development to fill the gaps necessary for nonlinear identification, but does not extend to recommendation or critical comparison of any of these. The purpose of the current paper is to describe a specific worked example test case to explore the more advanced and more promising of these new techniques.

## 1.2 A New Approach

The procedure outlined in Ref [1] comprises a series of 10 steps grouped in 3 Phases, as can be seen in Figure 1: Phase I **Preparation** – preparation for a nonlinear model validation process, including derivation of a validated Underlying Linear Model (ULM); Phase II **Test and Identification** – of the primary nonlinear features in the test structure, also referred to as Modal Test+; and Phase III **Verification and Validation** extending (i.e. upgrading) the model to include the necessary additional parameters, and then validating these by updating the coefficients for the additional model features. Full details can be found in ref [1] and will not be repeated here.

One of the main features of the proposed methodology is the formalisation of how the nonlinear characteristics are to be included in the model. This cannot be achieved by increasing the number of elements in the model mesh but, rather, by

increasing the complexity and order of each relevant element, and the number of parameters that are required to describe the nonlinear characteristic appropriately. Only when the model has an adequate set of parameters it can be subjected to an updating procedure whose role is to determine the most appropriate numerical coefficients for this model.

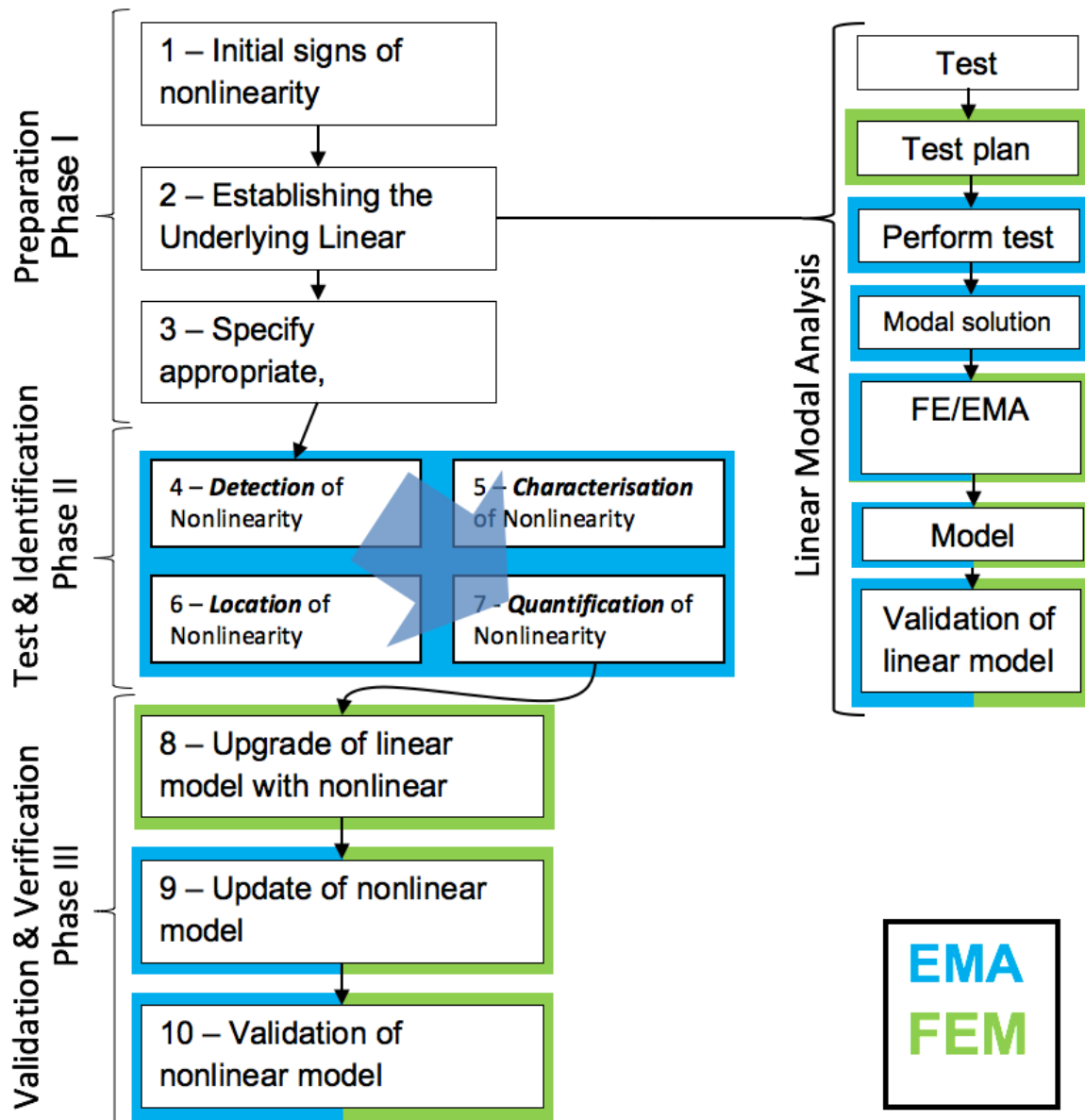


Figure 1 – Schematic representation of the proposed Modal Test+ procedure.

Another representation of the new procedure – more focused towards the data flow – is given in Figure 2 (the word “nonlinear” being abbreviated in NL).

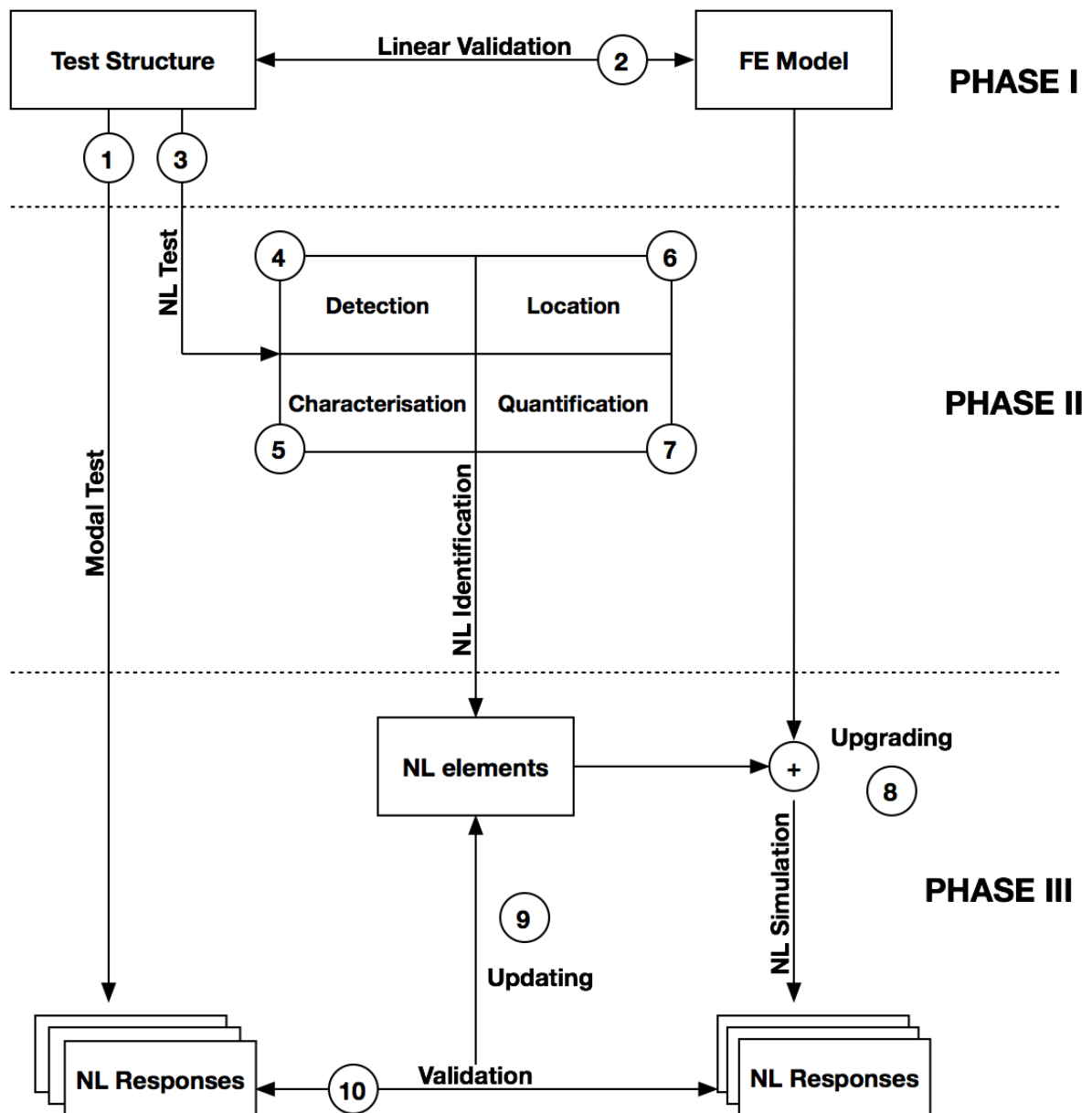


Figure 2 – Data flow scheme of the new procedure. The figure shows the three fundamental phases and each step is highlighted by a numbered circle.

### 1.3 Structure and Objective of the Paper

The structure of the paper is straightforward, and is as follows. Following introduction to the chosen test structure, and its features, each of the 10 steps shown in Figure 1 is undertaken in turn using methods that are often only available in

a basic, or research-level, stage of development. The objective is to explore the potential for achieving the required model validation capability for structures with nonlinearities, rather than to propose or to advocate specific numerical methods for the various stages. The results are then discussed, and conclusions drawn regarding the need for further development of crucial parts of the procedure.

## **2 Approaching the Structure: the Underlying Linear Model (Phase I)**

### **2.1 Introduction to Phase I**

Phase I starts with a conventional (i.e. linear) model validation procedure and is the stage at which the prospect is first raised of the possible need to conduct a more advanced validation process because the structure is suspected to be insufficiently linear for a traditional linear model validation to be effective. If signs of nonlinear behaviour have become evident in the course of this activity, then additional care is usually taken in the acquisition of the test data to be used for the validation process to minimise the risk of this being contaminated, or distorted, by the nonlinearities. Generally, the linear model validation proceeds at levels of vibration that are low enough to inhibit significant influence of many typical nonlinear effects. From this approach, it is usually possible to extract an Underlying Linear Model (ULM) that is intended to represent the structure under conditions where the nonlinear features are inactive.

After this is completed, attention is turned to the levels of vibration that are anticipated to apply at the service operation condition for which the model is required to be validated.

### **2.2 The Test Structure**

The illustrative case study given here was performed on a test rig intended to represent a wing and pylon structural subassembly, comprising an aluminium plate and a steel mass attached underneath the plate (see Figure 3). This rig was chosen because, while being relatively simple, it represents an abstraction of a genuine aerospace configuration. The pylon was suspended on two spring-steel rulers, which were rigidly clamped to the pylon mass and beneath the wing. The clamping at the wing was within a tapered slot, such that the rulers would increasingly contact the walls of the slot when displacement of the pylon was large, thereby shortening the pylon arm and causing a stiffening effect. The structure was suspended from a frame by four soft springs, and excited by a single shaker from beneath the wing.

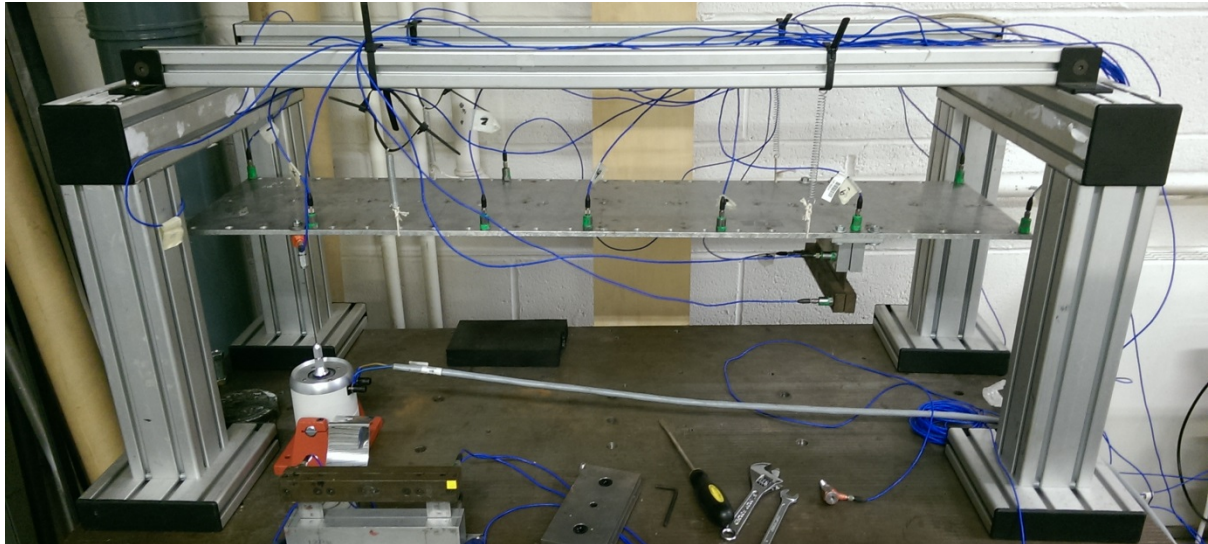


Figure 3 – Photograph of the instrumented wing-pylon structure

The sensors comprised 13 accelerometers and a force transducer (Figure 4). All signal acquisition was performed using National Instruments cDAQ hardware to allow for the capture of long time histories at a high sampling frequency (120 seconds at 10.24 kHz). The sampling rate was allowed to be higher than necessary for the frequency range of interest ( $<100$  Hz) in order to permit analysis of any higher harmonic content (including enough samples/cycle of the harmonics to permit investigation of the time histories). The random excitation spanned 0-1 kHz to provide persistent excitation at the frequencies in which harmonics of resonances may be found, and to capture residual content above the frequency range of interest.

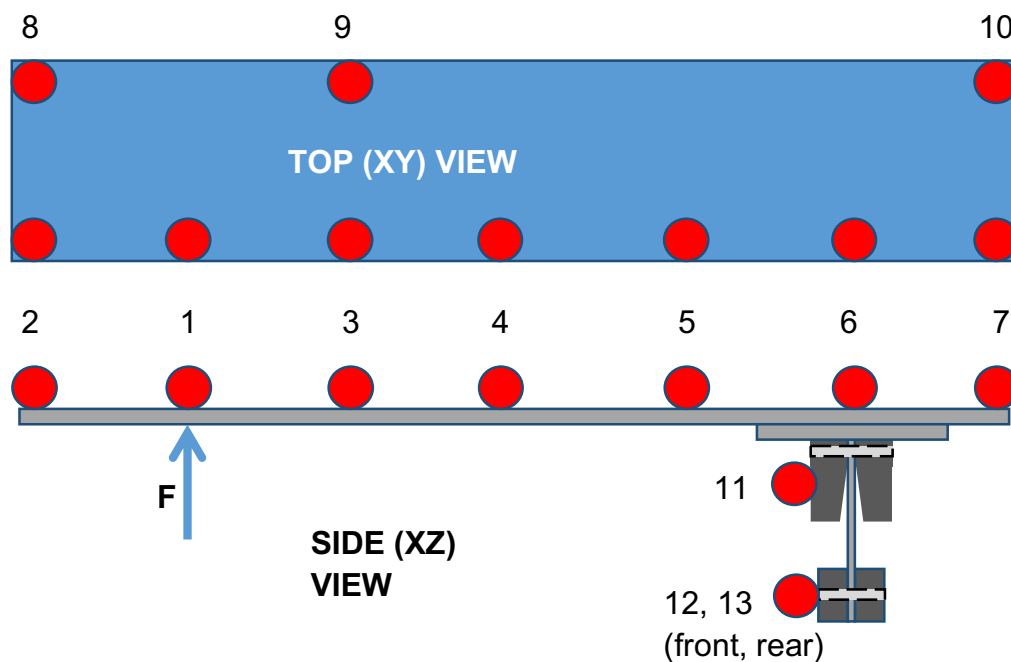


Figure 4 – Schematic of the wing-pylon structure, with sensor locations (circles) and excitation direction (arrow). DOFs 1-10 were aligned in  $z$  (wing out-of-plane direction) and DOFs 11-13 in  $x$  (wing longitudinal direction)

### 2.3 Measurements on the Test Structure

The first measurements taken on the test structure consisted of several Frequency Response Functions (FRFs) using broadband excitation, as is typical in conventional modal testing because this provides early feedback on the nature of the structure and possible problems with the test configuration. The FRFs (and associated coherence functions) also give an indication as to whether the structure can be assumed linear. Random excitation was used here and has the effect of averaging the FRF over multiple excitation levels, and so the shape of the peaks can appear classical (i.e. linear). However, by taking data at low- and high-level excitations, frequency and amplitude shifts in the FRF corresponding to softening or stiffening are still observable, and are the basis for the homogeneity method for detection of nonlinearity. In Figure 5 we see some shifts in the resonance frequencies, particularly for the measurements on the pylon. In Figure 6 we observe reductions in the coherence function, particularly for the pylon around 100 Hz, which are likely to be attributable to the harmonic content of a lower-frequency resonance, although at this stage it is unknown which resonance this is.

Stepped-sine excitation is the simplest excitation that can be input to a nonlinear system and, by maintaining the input level for all excited frequencies, amplitude-dependent nonlinearities can be emphasised. Step-sine excitation is, however, slow – particularly whilst maintaining a nominal input or output level – and therefore an unnecessary expense for the linear case wherein the step-sine FRFs are the same as those using any broadband excitation. The step-sine data were acquired using the NI cDAQ hardware by implementing a simple rolling buffer to provide feedback control. The amplitude of the sinusoid sent to the shaker was updated to achieve the desired input force levels to within  $\pm 10\%$  of the nominal desired input level. In order to track potentially unstable branches of the FRF as far as possible, sharp transitions in the output were minimised between buffers by (i) preserving the phase and (ii) use of a relaxation factor when amplitude was altered. Only the fundamental frequency of interest was controlled, neglecting harmonic content fed back to the shaker and present at the accelerometers. This was because the dynamics of the structure appeared strongly dependent on the pylon; since the pylon could only be indirectly influenced by the shaker through the wing, in this case it was found that multi-harmonic control [2] tended not to converge, or provided a worse input sinusoid than without multi-harmonic control.

In Figure 7 stepped-sine FRFs are given, each focused around a resonance of interest, and at the lowest and highest input levels that could be achieved (limited by signals acquisition at low input levels and fixturing of the test-rig at high input levels). These step-sine FRFs neglect all higher-order content (on both input and output), and are effectively a targeted (single frequency) Discrete Fourier Transform (DFT) (for their calculation see [3]). The driving point on the wing and a measurement on one end of the pylon are given, since different behaviour is observed on each component. For the first resonance (top row) over the tested input range we observe



the pylon to soften by a factor of approximately two, whilst the peak response frequency increases. The resonant peak leans to the right, causing a sudden transition (jump) down to a lower energy state when increasing in frequency, and a smaller transition up to a higher energy state when decreasing in frequency. At the driving point the peak response frequencies are also increased at higher input levels, but a transition from a high energy state to a low energy state is observed for both increasing and decreasing frequencies. The second resonance (Figure 7, second row) appears less strongly nonlinear, although again the accelerances at the pylon and driving point do not scale together (the pylon softens more). It is unsurprising for local nonlinearities that some of the resonances are appreciably more nonlinear than others, as the participation of the nonlinear element(s) will be different for each deflection shape.

The step-sine FRFs may provide some characterisation of the nonlinearity(ies) over the initial homogeneity check, but their primary purpose here is to provide a dataset for validation of the nonlinear FE model. Although not discussed here, the nominal low-level mode shape information was also provided by this dataset (i.e. gross spatial behaviour of the structure, but not a strictly-defined linear eigensolution). Note that performing such tests at both low and high levels can induce nonlinear effects that should not be confused with the structural nonlinearities, particularly signals issues like Signal-to-Noise Ratio (SNR), dynamic ranges, sensor cross-sensitivities, or the fixtures and suspension that hold the test structure and the exciter. For test structures that behave with significant amplitude-dependent nonlinearity, even the  $\pm 10\%$  tolerance on the desired input level can appreciably distort the FRFs, and was the cause of the small spikes observed in Figure 7.

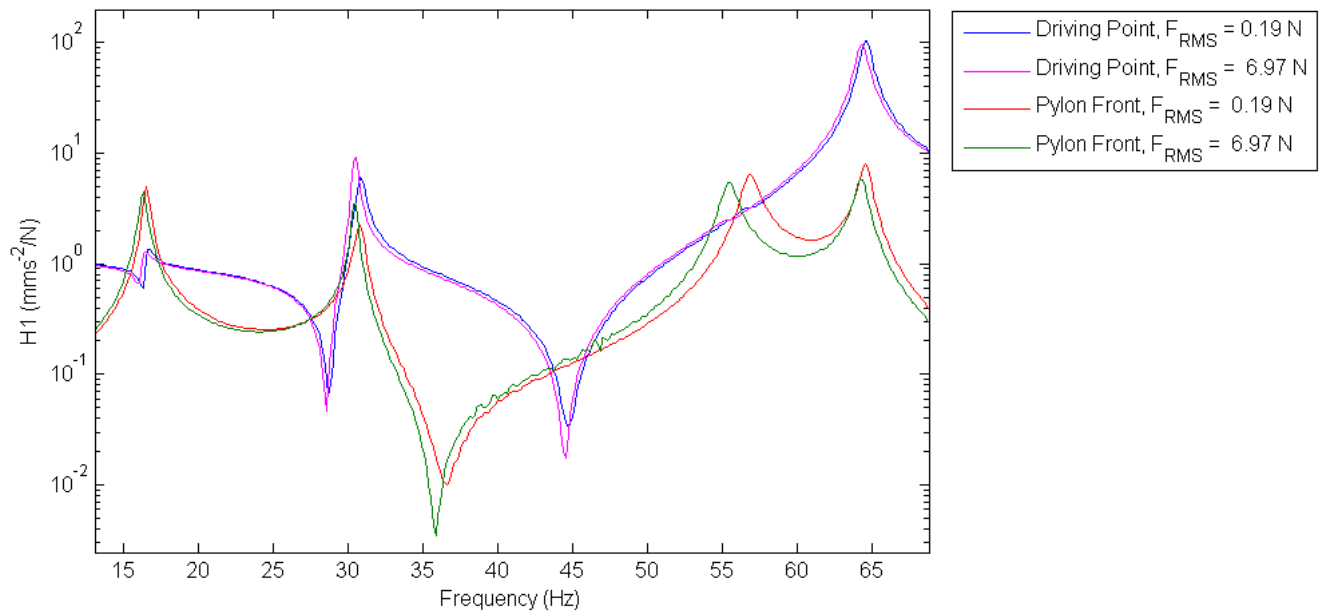


Figure 5 – FRFs from the driving point and pylon, taken using random excitation at low and high excitation levels.

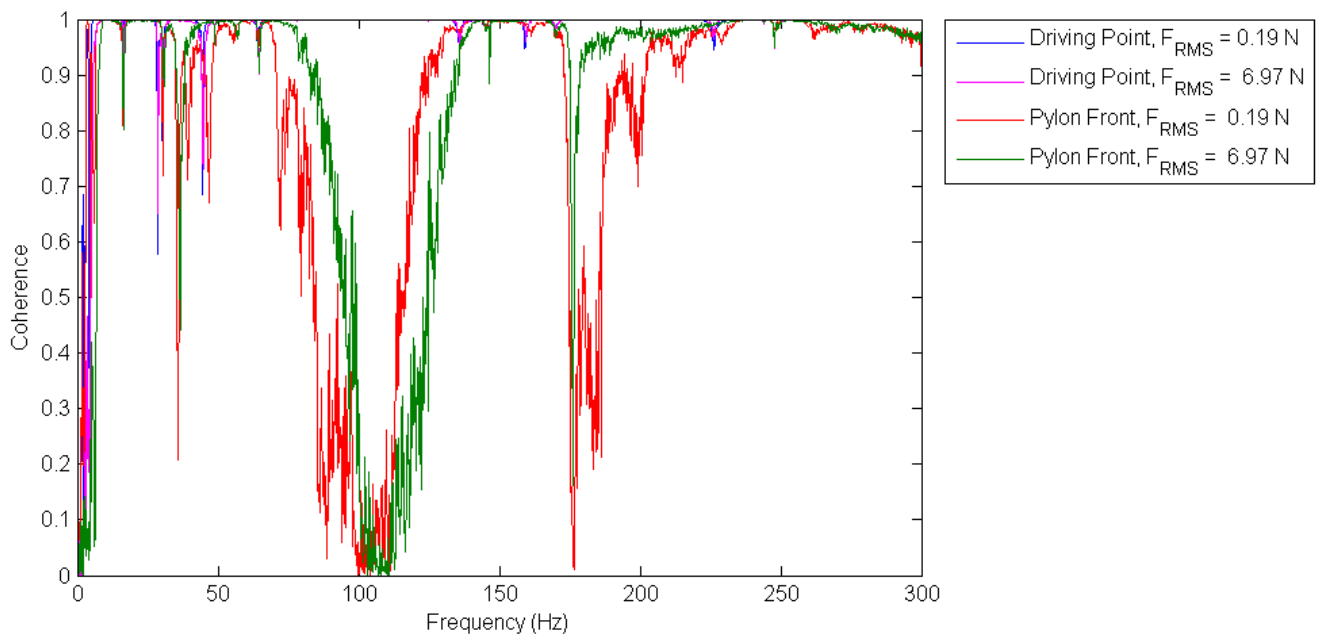


Figure 6 – Coherence for the driving point and pylon. Note that a broader frequency range is considered in order to include harmonics of the frequencies of interest.

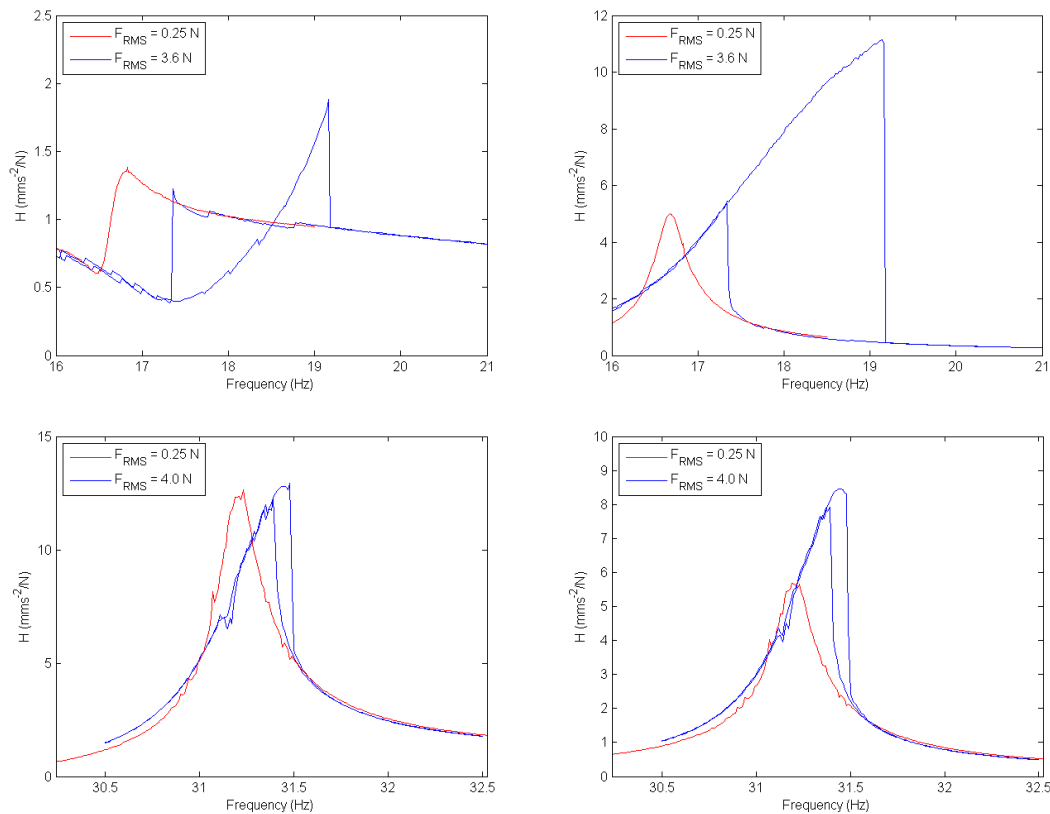


Figure 7 – FRFs for driving point (left column) and pylon (right column), taken using constant-input step-sine excitation. These resonances were pylon local  $1F$  and wing-pylon  $1F-1F$ .

## 2.4 The Preliminary Linear Model

Since it is supposed that the structure is essentially linear with the prospect of a few nonlinear elements, it is necessary first to validate our mathematical model in the linear regime, so that it can be augmented later with nonlinear elements (in a process which we refer to as *model upgrading*). As the test structure consists largely of a plate, it was modelled mathematically by means of finite shell elements (Figure 8). The suspension was modelled by means of four 3D springs to achieve a good agreement in the boundary conditions. In order to keep the model simple yet capable of describing the general dynamical behaviour, the connections of the pylon to the wing were modelled by kinematic constraints, and the main inertias of the pylon concentrated in a single point. The materials were aluminium for the wing and immediate under-wing assembly, steel for the mass of the pylon and spring steel for the connecting flexural springs. The tapered slot in which the springs reside was not modelled geometrically, with its effect to be accounted for later during the model upgrading stage (Section 4.3). The FE model was generated using commercial software ABAQUS by Dassault Systemes and is shown in Figure 8.

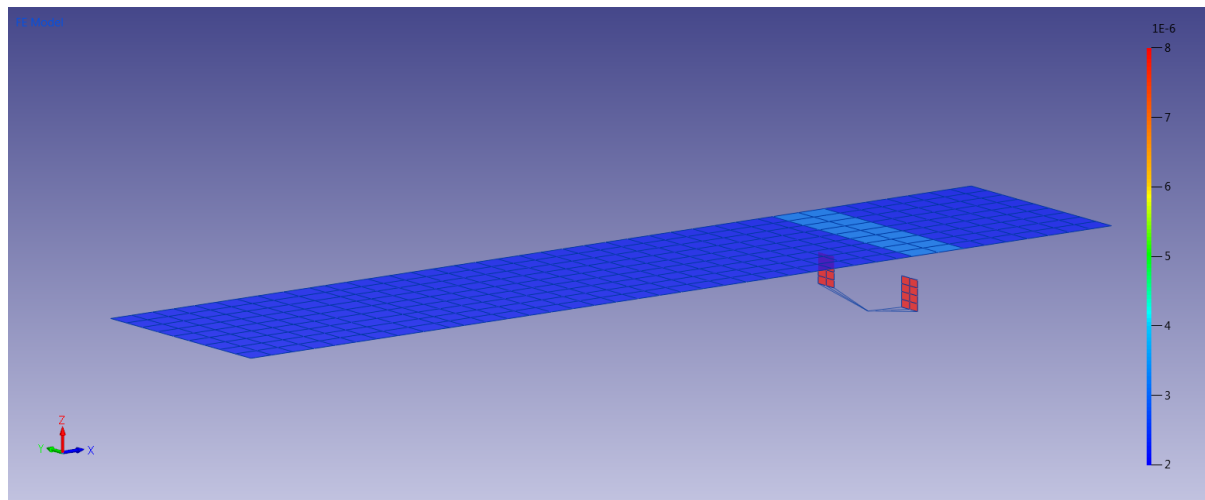


Figure 8 – FE model of the wing-pylon structure

## 2.5 Test-Analysis Correlation

The initial FE model was then correlated and updated against the low level random excitation modal test in order to provide the correct natural frequencies and mode shapes (MAC values) for the first 6 modes, over a bandwidth of 100 [Hz]. Since the primary unknowns were the specific material parameters, a greater margin was permitted for their values to change (10%), while the shell thicknesses and mass information of the pylon were constrained to variations of 3% at most. The updating was carried out using the FEMtools package by DDS. The results of the updated model are found in Table 1, while Figure 9 shows some updated mode shape pairs. The final outcome of this process provides what is referred to elsewhere as the Underlying Linear Model (ULM).

Mode#	Description	FEA [Hz]	Test [Hz]	Diff [%]	MAC [%]
1	Rigid	4.66	4.70	-0.72	84.1
2	Rigid-1F	16.79	16.75	0.21	94.6
3	1F-1F	32.53	31.24	4.10	96.7
4	Rigid-1T	57.75	57.80	-0.07	91.8
5	1T-1T	69.58	66.04	5.36	98.0
6	2F-1F	86.65	80.22	8.01	96.2

Table 1 – Updated FE model natural frequencies and MAC values.

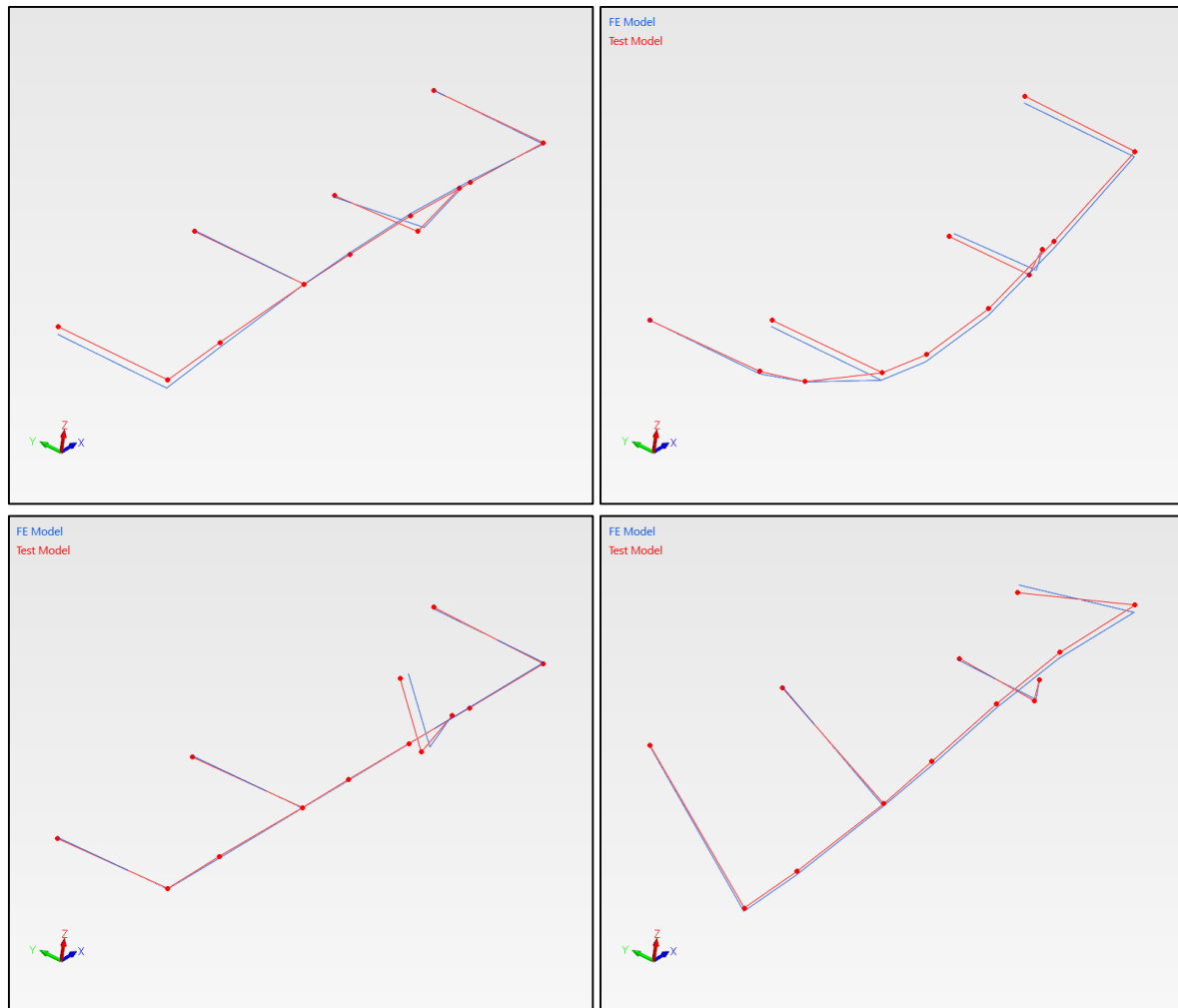


Figure 9 – Some mode shape pairs for FE model and test: mode 2 (top-left), mode 3 (top-right), mode 4 (bottom-left), mode 5 (bottom-right).

Figure 10 shows comparisons between the measured response levels at two levels of excitation (dots) and predicted responses using the linear FE model. Despite the relatively successful linear validation procedure, and the good prediction of response at low excitation levels, it is clear that the linear model is not an acceptable representation of the structure's behaviour in the regions of high response levels at resonance. While the model correctly reproduces test frequency response data in the desired bandwidth at low levels of excitation, its intrinsic linearity causes the inability to reproduce test frequency data at higher force levels due to the lack of nonlinear features.

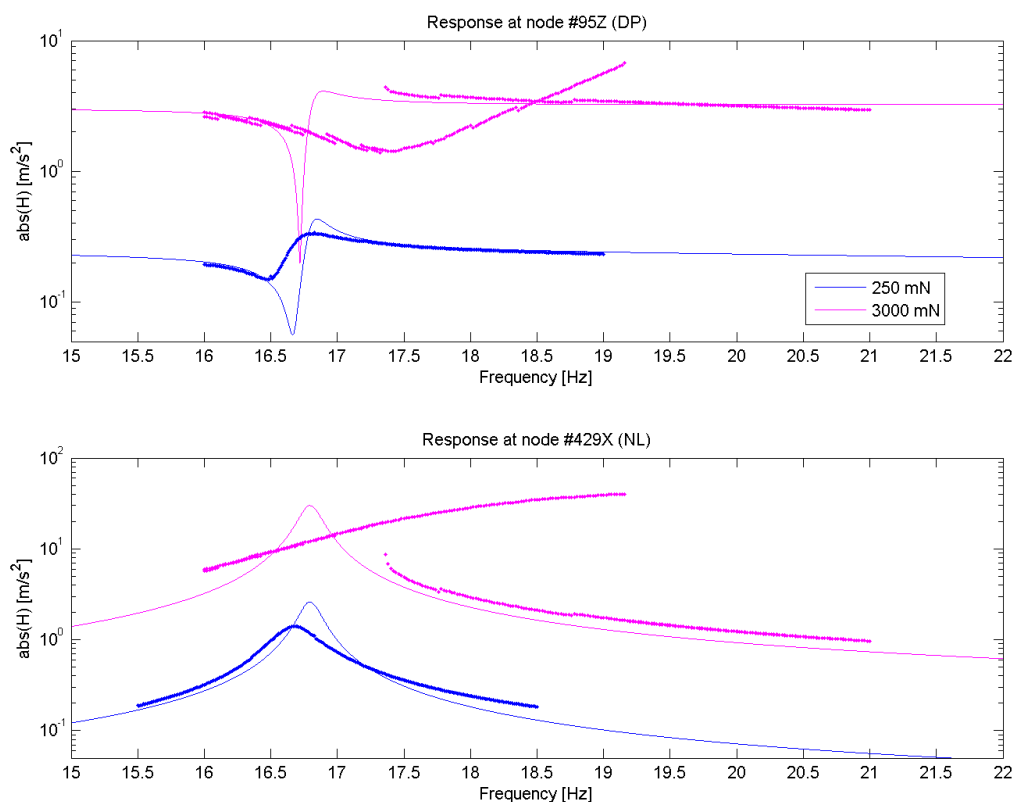


Figure 10 – Comparison between acceleration levels for driving point (top) and pylon (bottom). Two force levels are considered. The error between the test (dotted line) and the underlying linear model (solid line) increases with the force level.

## 2.6 Summary of the Results from Phase I

In implementing Phase I of the proposed procedure, we have applied conventional modal testing and model validation procedures to the test structure. We have found that with a relatively simple FE model, it is possible to describe the dynamic response characteristics of the test structure with an acceptable<sup>1</sup> accuracy – including, most importantly, the response characteristics – when exciting the structure at low levels of force. The updated model constitutes the Underlying Linear Model (ULM) for this test structure. In contrast, when the excitation forcing is increased by an order of magnitude, the same ULM is clearly not capable of describing the dynamic behaviour of the same test structure at these conditions. The indications are clear that the discrepancy at higher levels is associated with a nonlinearity and is

<sup>1</sup> We accept that we have not defined or discussed ‘acceptable accuracy’. This is an issue of a practical judgement that must be made in each specific case, depending on a wide range of factors – many of them not related to details of the test structure itself. It is common practice to regard MAC values in excess of 80% to be ‘acceptable’ while the accuracy of natural frequency predictions depends heavily on the nature of the excitation. In this case, it would be expected that the vibration problem of greatest concern here would be associated with the two fundamental modes and here a discrepancy of less than 1% is considered to be ‘acceptable’.

unacceptably large, and so Phases II and III are necessary to identify the nonlinearity and to introduce it into the initial linear model.

### **3 Identification of Nonlinear Elements (Phase II)**

#### **3.1 Introduction to Phase II**

The core nonlinearity identification procedures are performed in Phase II. Here, new measured response function data are acquired under more closely-controlled excitation conditions, chosen to ensure that the structure is exercised at vibration amplitudes representative of those anticipated in service. The overall objective of Phase II is to locate and identify those parts of the structure that exhibit nonlinear behaviour. The nonlinear elements need to be individually identified so that appropriate enhancements (upgrades) can be made to the model to ensure the nonlinear behaviour is captured and described by the enhanced model. Four distinct aspects of the identification are addressed – Detection, Characterisation, Location and Quantification – although some identification algorithms will address more than one of these at a time. The rationale of the D-C-L-Q sequence is that successful characterisation of the nature of the nonlinear effects (stiffness and/or damping) might assist the location task. Quantification naturally follows successful completion of the previous tasks.

It should be noted that care must be taken at the measurement stage to ensure that it is made clear exactly what form of ‘response function’ is obtained. Strictly, the specific excitation signal used must be specified and care taken when deriving response functions for nonlinear structures.

#### **3.2 Detection**

*Detection* indicates that some effect attributed to nonlinearity is observed, and it is deemed that a standard linear model cannot adequately represent the system response. The detection process should deliver more than a mere linear/nonlinear indication. It should indicate which line of action should be undertaken in order to address the observed nonlinear behaviour most effectively (e.g. based on detection, one could consider fully characterising the nonlinearity, linearising it around a suitable working point, or completely neglecting it).

The first and most noticeable indicator of nonlinear behaviour is a lack of homogeneity in frequency response functions over different force inputs. By looking at Figure 7 it is immediately obvious that the structure behaves differently for different input forces, in contrast with established linear theory. The shifts in frequency and amplitude of the FRFs were here deemed not to be safely negligible, and we require a full identification of the nonlinearities. In order to do so, one must address each of the fundamental properties that define the nonlinear elements to be included in the system: location, characterisation and quantification.

### 3.3 Location

*Location* refers to determining exactly where the nonlinear features are positioned in the spatial description of the structure. In mathematical terms, this means identifying which of the DOFs in the model are closely located to the source of the nonlinear behaviour.

Discrete nonlinearities are located at the interface between two components and are responsible for the majority of their nonlinear behaviour (e.g. joints). These can be modelled by spring/damper elements with higher-order characteristics and are differentiated in the ‘grounded’ or ‘non-grounded’ variety, depending of the number of degrees of freedom they involve. A grounded nonlinearity is a function of the absolute displacement/velocity of a single degree of freedom, while a non-grounded nonlinearity is function of the relative displacement/velocity of one degree of freedom with respect to another. Grounded nonlinearities are mostly found between the test structure and its fixture while in general the nonlinearities can be regarded as non-grounded (e.g. acting across a joint between two components of the structure).

Of course, one must be aware that no method can provide reliable location information if the test geometry does not contain DOFs near and/or across the cause of the nonlinearity. Although this might seem a major issue, the engineer can usually narrow the range of possible locations in which nonlinearities are expected to be found, based on experience or common assumptions (e.g. joints play an important role in nonlinear behaviour for assembled structures). In this specific case, we were aware of the location of the nonlinearities, since the structure comprised primitive elements coupled through a carefully designed joint.

A simple and often unconsidered method to locate nonlinear elements is to check the coherence levels of data measured at each degree of freedom, looking for any abnormal loss. In this regard, it is useful to define a ‘coherence index’ as the normalised integral of coherence in the reference bandwidth:

$$\kappa_i = \frac{\int_{\omega_1}^{\omega_2} \gamma_i(\omega) d\omega}{\omega_2 - \omega_1}$$

Where  $\gamma_i$  is the coherence of degree of freedom  $i$  and  $[\omega_1, \omega_2]$  is the reference bandwidth. Each DOF  $i$  then yields an index between 0 and 1 that indicates the quality of its coherence in the reference bandwidth. For the structure under investigation, the coherence-check (Figure 11) shows that the most affected DOFs are #12 and #13, located on the pylon, across the nonlinear springs.



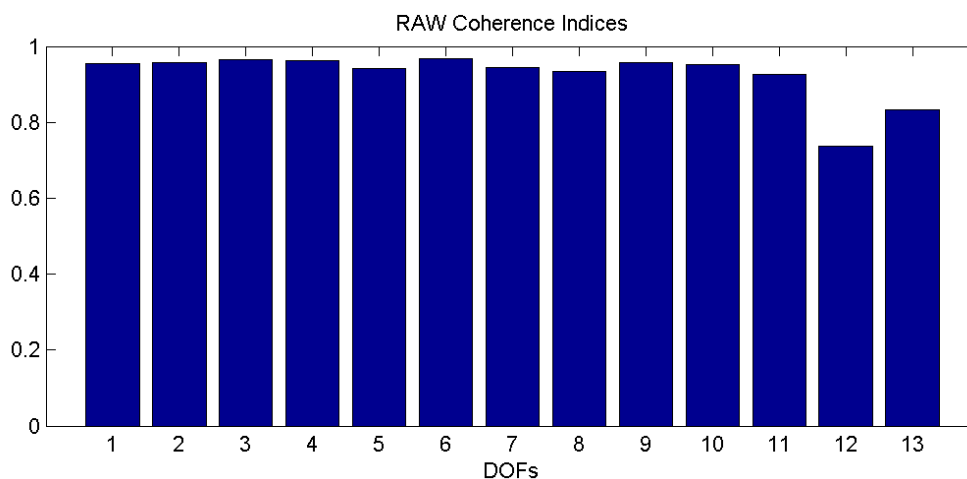


Figure 11 – Coherence Indices across all DOFs (0-300Hz). The degrees of freedom sitting across the Joint are the ones that experience the most severe coherence losses.

Some drawbacks to this kind of check are the inability to assess whether the nonlinearity is grounded or not, or to indicate how many nonlinearities are present and between which DOFs they are acting. In addition, its performance is heavily affected by low SNR measurements, especially where SNR varies significantly at different DOFs (e.g. where a mixture of accelerometer sensitivities are employed).

### 3.4 Characterisation

The most important aspect that the engineer must address in a nonlinear identification is the identification of which aspect(s) of motion drive the nonlinear behaviour (e.g. displacement, velocity), how the nonlinear effect might need to be described functionally (e.g. polynomial, multi-linear) and what are the parameters of the functional (e.g. exponents of a polynomial). All these properties define the 'character' to the nonlinear behaviour, and are referred to together as *Characterisation*.

One of the methods that can potentially deliver a thorough set of nonlinear elements is the *Reverse Path* method (RP) and its conditioned form (CRP). Originally introduced in [4] and further developed in [5] [6] [7] the RP is based upon the analysis of a signal measured using random excitation and treats nonlinear terms in the equations of motion as input feedbacks, constructing a set of linear Multiple-Input-Single-Output (MISO) systems with the force at the output and both linear and nonlinear displacements/velocities at the input. These MISO systems can then be studied with conventional linear techniques in order to retrieve the nonlinear elements that best describe the experimental data. More technical information can be found in the short appendix to this article.

In order to do this, the trial nonlinear models (comprising the linear system with an additional functional characteristic and location) are computed one at the time, and the resulting coherences are assessed against the standard 'raw' coherences. The nonlinearity from the trialled model that delivers the best coherence improvement is used to upgrade the ULM, and a second iteration of model upgrading can then start.

By spanning the whole space of possible locations and characteristics, it is possible to assemble nonlinear elements with multiple parameters, and in different locations of the FE model. The method relies on 'brute force' calculation of all desired trial nonlinearities at all locations (between DOFs, or a DOF and ground), and so presents a computational burden.

We perceive the strength of the reverse path method to lie in its ability to characterise nonlinearities in systems with a modest number of DOFs, say 10-12 DOFs using a standard desktop computer. The RP method has some ability to locate nonlinearities, but in our experience tends to work on a 'component' level, i.e. locations for the nonlinearity are posited, but are limited by the necessarily relatively sparse test geometry (to ease the computational burden). Therefore the model will usually not have DOFs spanning the nonlinearity unless it is already known/suspected (in which case the reverse path method may only add corroboration to locating the nonlinearity). The identified DOFs may also be implausibly misaligned (i.e., the added NL element may act between completely unaligned DOFs in a way which appears abstract/non-physical).

RP method is a useful tool for characterisation of nonlinearity, which is arguably the most challenging part of the Modal Test+ DCLQ framework. It also provides quantification in the form of a spectrum of coefficients, but in practice the spectrum yielded is typically ill-defined. Once the characteristic of the nonlinearity is established, we recommend use of another method for quantification, such as frequency nonlinear subspace identification, structural model updating, or the conditioned reverse path method.

Three successive trial model upgrades are shown in Figure 12. In the first iteration there is observed to be a lot of content (i.e. potential improvement to the model) by inclusion of an  $x^3$  term. This is strongest for 6-12 and 6-13, which are the DOFs above the pylon in  $z$  (DOF 6) and at each end of the pylon in  $x$  (DOFs 12, 13 see Figure 4). Such a cubic stiffness is somewhat difficult to envisage since it acts between perpendicular degrees of freedom, and it falls to operator knowledge whether to include such a seemingly non-physical/contrived spring in the ultimate upgraded FE model, or whether to take the  $x^3$  nonlinear element and bridge DOFs 11-13 (both in the  $x$  direction). Nonetheless, permitting the  $x^3$  element between 6 and 12, a further model iteration indicates an improvement in coherence by inclusion of an  $x^5$  element also between 6 and 12, then further a  $x^7$  element also between 6 and 12. Notably, the second and third trial updates are more clear-cut and consistently locate the nonlinearity. The coherence before and after upgrading the model are shown in Figure 13 **Error! Reference source not found..**

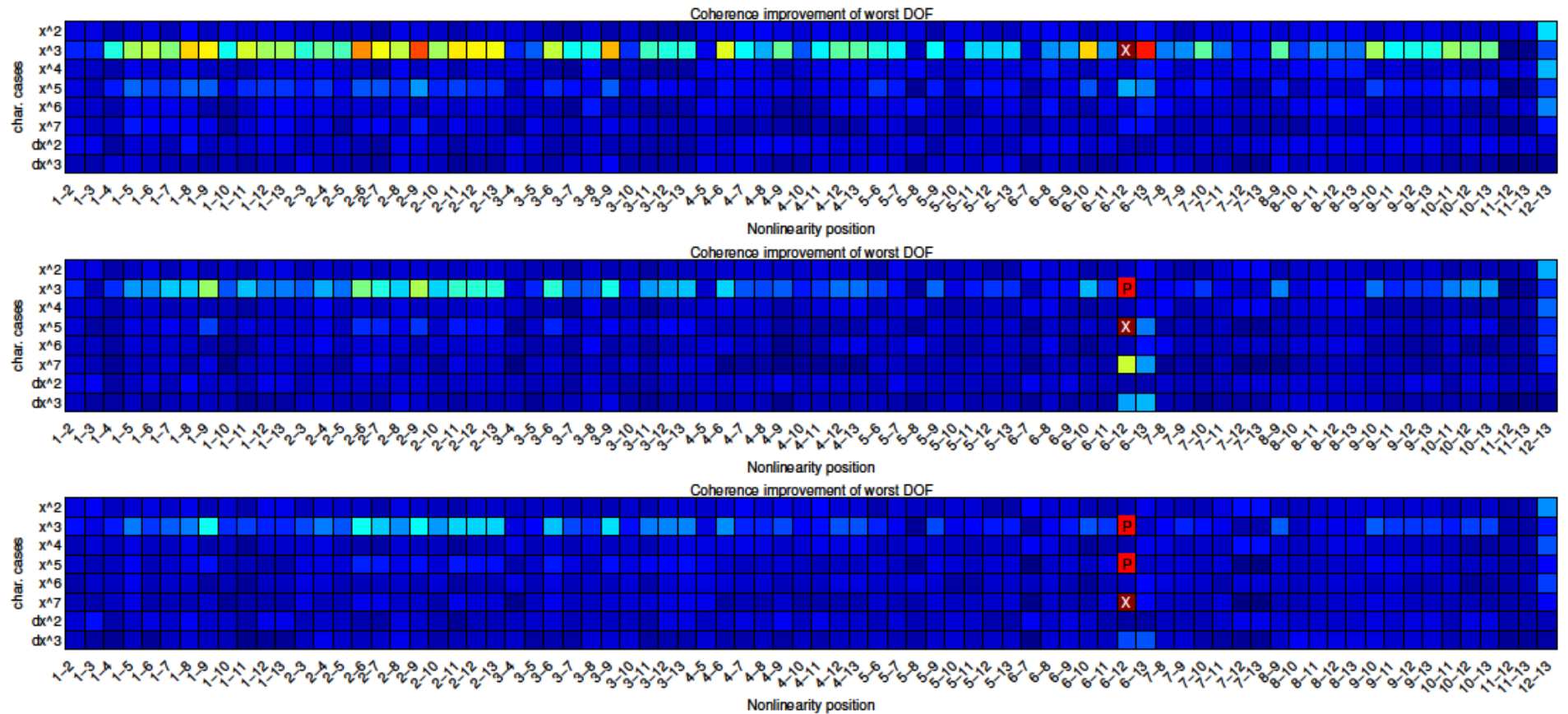


Figure 12 – Three successive reverse path iterations, chronologically from top to bottom. The trial upgrades consistently place the nonlinearity between DOFs 6 (wing, above the pylon) and 12 (pylon), and the included model upgrades were the  $x^3$ ,  $x^5$  and  $x^7$  stiffness characteristics. 'X' indicates the selected nonlinear element, while 'P' indicates elements previously added to the upgraded model.

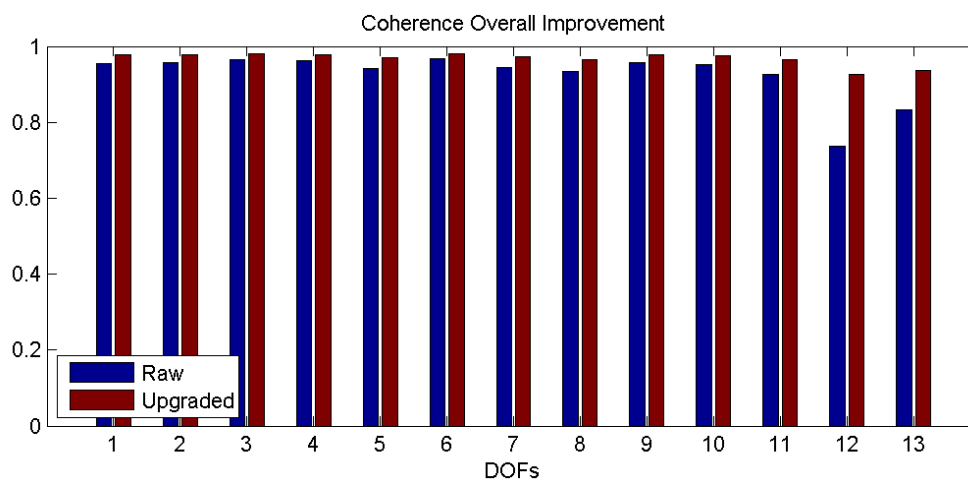


Figure 13 – Coherence improvement across all DOFs, after model upgrading.

In order to test the stiffness characteristic identified by the Reverse Path analysis, the pylon was removed from the wing-pylon rig and installed in a static tensile test machine (note that this would also be a useful characterisation for Modal Test+ without RP analysis). The resulting static restoring force characteristic for the pylon is given in Figure 14 with a best-fit for the  $a_1x^7 + a_2x^5 + a_3x^3 + a_4x$  characteristic from the Reverse Path analysis from dynamic testing also given. The fit is observed to be fair, and significantly better than a simple first-order fit. It is notable that further model upgrades using the reverse path method (not shown here) advocated inclusion of even-numbered polynomial terms between 6 and 12 and, as would be expected, this improved the fit between the identified polynomial stiffness and the static tensile machine test. The even polynomial terms accounted for the asymmetry of the pylon restoring force characteristic, because the tapered slot was slightly non-symmetric. Ultimately, however, these even terms were not included in the updated model as it was considered potentially over-fitting, and it was desirable to probe how representative the updated model would be without these terms, since a generic model representative of a fleet of structures is typically desired (and one would assume the asymmetry not intentional). Note that the range of displacement in the static test is significantly larger than that observed within the dynamic tests ( $\approx \pm 6.5\text{mm}$  vs.  $\approx \pm 2\text{mm}$ ); this was considered best practice because: (i) in simulations from the FE model a greater dynamic range may be required than was tested dynamically, which would be dangerous to extrapolate and (ii) polynomials are known to be potentially less accurate toward the ends of the interval, suffering from Runge's phenomenon [8].

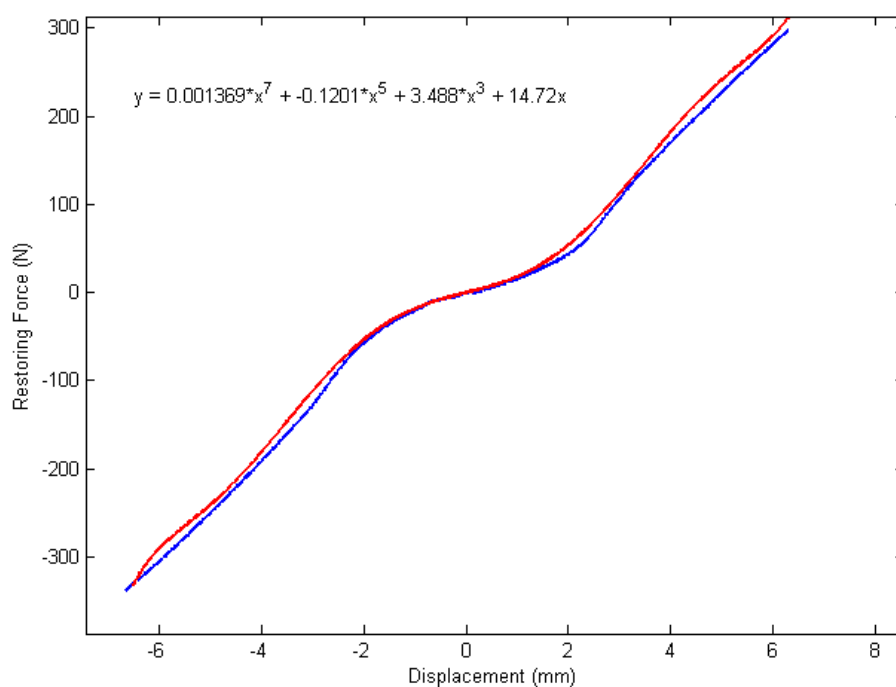


Figure 14 – Static Test (blue) vs. Polynomial Fit (red).

### 3.5 Quantification

The last step in order to define the nonlinear elements thoroughly is identification of the coefficients that give the required effect in the equation of motion. *Quantification* refers to the search for the correct numerical values of each scaling factor (coefficient) associated with a previously-characterised nonlinear term.

In order to do this, one could use quantification methods like the Frequency Nonlinear Subspace Identification [9] or the Conditioned revision of the Reverse Path method [6] or, alternatively, just assume some reasonable starting coefficients and feed them into an unconstrained nonlinear optimiser algorithm, like the Nelder-Mead's simplex direct search [10] (i.e. quantification by model updating).

In this case, the values retrieved by the polynomial fit of the static test were used as starting coefficients for the main updating loop.

### 3.6 Summary of Results from Phase II.

Phase II contains the major activities which have to be undertaken in this attempt to capture a valid description of the nonlinear physical characteristics which the structure possesses.

Measurements have been made of forced random vibration of the structure and the resulting data analysed using Reverse Path method. The location of the strongest nonlinearity in the test structure – which was always visually evident – was confirmed by this analysis, with no other significant regions being revealed in the process. Both the dynamic tests, and a static test using a static tensile test machine, agreed closely

on the form of nonlinear characteristic of the crucial part of the structure. Thus, the essential result from Phase II was the correct location of nonlinear components in the test structure, and identification of a polynomial stiffness characteristic for those components.

## **4 Model Upgrading, Updating and Validation (Phase III)**

### **4.1 Introduction to Phase III**

Phase III is the least mature phase of this new procedure. The three steps (8, 9 and 10) are clearly defined, but the means of carrying them out are not as well developed as the other Phases. The first step, 8, concerns the upgrading of the initial (and, presumably, linear) model by introducing the additional parameters which are necessary to describe the nonlinear stiffness and/or damping effects that are present in the structure. Put in the simplest of terms, it is to implement the higher-order elements which are deemed necessary to capture and describe the nonlinear effects, as these are invariably amplitude dependent (as opposed to amplitude independent in linear systems). Once these additional elements have been incorporated, Step 9 can be carried out to optimise the numerical values of all the new parameters now in the model, in an extension of the model updating process carried out routinely in linear model validation. The last step, 10, is undertaken in order to demonstrate the validity of the upgraded and updated model by using it to predict, and then to measure, the behaviour of the structure in a different configuration, or under different loading to that used in the overall validation exercise. Achieving an acceptable level of agreement between these predictions and subsequent measurements on real hardware provides the necessary evidence for the overall validation process.

### **4.2 Model Validation for Nonlinear Models**

Model Validation is the process of assessing the validity of a model. Dynamics models of structures in the linear regime often come in the form of systems of equations that can either be in physical form or in modal form, the difference between the two being a change of coordinates<sup>2</sup>. The major drawback of the modal form is that once the modal model for a test structure is found, it can only be used to describe the dynamics of that specific configuration. The modal model is therefore not able to predict the effect of design modifications as the physical information is lost. One example of this approach – applied to the Wing-Pylon test structure – can be found in [11], where the system is described with an elegant compact model that trades off in terms of maintenance and modifications.

---

<sup>2</sup> The coordinates associated with the modal form are commonly referred to as *modal coordinates* or *generalised coordinates*, as opposed to the standard *physical coordinates*.

A Finite Element model is a physical representation of the system of equations of motion (i.e. it has an associated geometry) and it is the industry standard for structural models. As a physical model, FE permits study of design modifications, which is not possible with modal or otherwise abstracted models.

In the linear regime, modal parameters of the test structure are always used as a paragon for the model, since natural frequencies, damping factors and mode shapes are all the information ever needed in order to inform a perfect linear model. When nonlinearities become significant, these modal quantities are not well-defined anymore, as they depend on other quantities like the amplitude of vibration.

The main objective of modal testing is to produce a model suitable to describe the system. When the structure fails to admit an acceptable modal form, the best way to validate the model is then to choose another suitable paragon for the nonlinear model. In the early years of structural dynamics, every model was correlated against the *receptances* (FRFs) of the real structure, so it is suggested that one tries to correlate the responses of the novel nonlinear models with their measured counterparts without the need to use further analysis tools.

### 4.3 Model Upgrading

We define the process of including the previously identified nonlinear elements in an existing model (usually a Finite Element model) as Model Upgrading, and this is necessary to allow the model to describe the nonlinear behaviour within a range of force levels. For the wing-pylon example, Model Upgrading was performed by manually adding the previously identified nonlinear elements into the system of equations from the FE model (Table 2) thus modelling the tapered slot as a set of nonlinear springs. In order to do so, the mass and stiffness matrices of the system were extracted and the nonlinear terms added to the equations. As an optional step, a model reduction scheme was applied in order to retain all the measured DOFs as well as the ones involved in the nonlinear terms (location). It is suggested that Dynamic Reduction [12] is used for a reduction on a mode-by-mode basis, or SEREP [13] for global reduction on large bandwidths. Finally, the model has also been upgraded in order to accommodate a coefficient for modal damping on a force-by-force basis.

Element #	location (dof1 – dof2)	character (model)	strength (coefficient) before updating	strength (coefficient) after updating
1	415x – 421x	$x^3$	300 [N/mm <sup>3</sup> ]	181 [N/mm <sup>3</sup> ]
2	430x – 436x	$x^3$	300 [N/mm <sup>3</sup> ]	168 [N/mm <sup>3</sup> ]
3	415x – 421x	$x^5$	-50 [N/mm <sup>5</sup> ]	-5.5 [N/mm <sup>5</sup> ]
4	430x – 436x	$x^5$	-50 [N/mm <sup>5</sup> ]	-5.5 [N/mm <sup>5</sup> ]
5	415x – 421x	$x^7$	1 [N/mm <sup>7</sup> ]	0.18 [N/mm <sup>7</sup> ]
6	430x – 436x	$x^7$	1 [N/mm <sup>7</sup> ]	0.18 [N/mm <sup>7</sup> ]

Table 2 – Nonlinear elements included in the upgraded FE model.

With the newly generated system of equations of motion, one can simulate a steady-state Frequency Response Function truncated at the fundamental harmonic by means of an harmonic balance technique [14] that can be later correlated with the acceleration responses retrieved from stepped-sine excitation, as shown in the plots in Figure 15.

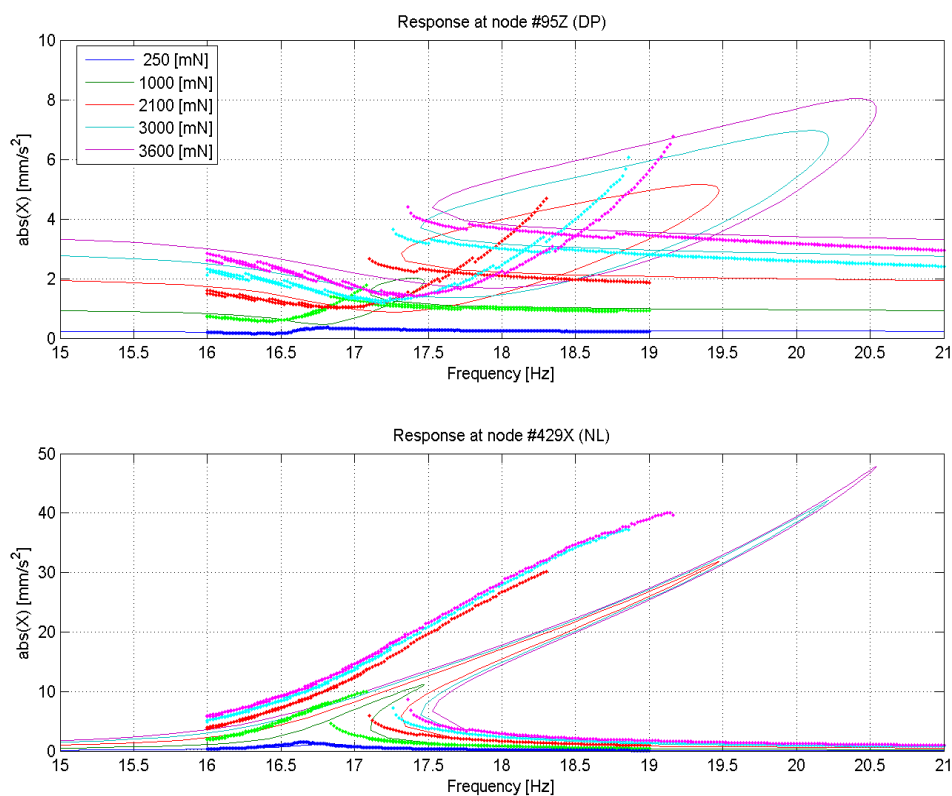


Figure 15 – Acceleration levels for driving point (top) and pylon point (bottom) across several force levels. Dotted lines are from experiments, continuous lines are from upgraded FE model, before updating (using starting coefficients).

Here we remind that while there are some in-house developed tools capable of simulating steady-state responses in the frequency domain [15], these tools are not available at a commercial level; thus an internally developed code based on the Harmonic Balance Method under a continuation scheme (named VIVALDI) has been employed for the simulation of the NL responses.

#### 4.4 Model Updating

After model upgrading the model remains inexact, but now has the necessary parameters to describe the nonlinear behaviour that can be observed in the measurements, as we demonstrate in this section.

It is worth pointing out first that different models will need different coefficients for the same nonlinear characteristics in order to accurately match the measured data. A shell elements model with kinematic constraints and lumped masses, as in this case, will require different coefficients than a solid elements model where the joint is more



accurately represented. However, this is true for the coefficients only, since the characteristic of the nonlinearities (the functionals that relate two degrees of freedom) will likely remain the same across the modelling space since the nonlinear functionals were informed by a physical basis.

In order to make the model match the real data, it has to pass through a mathematical optimiser that minimises the error function by iteratively changing the coefficients of the nonlinear parameters.

The optimiser used in this case was the Nelder-Mead simplex direct search in its MATLAB implementation. After some iteration, the response from the updated model was observed to correlate well with the test data (Figure 16).

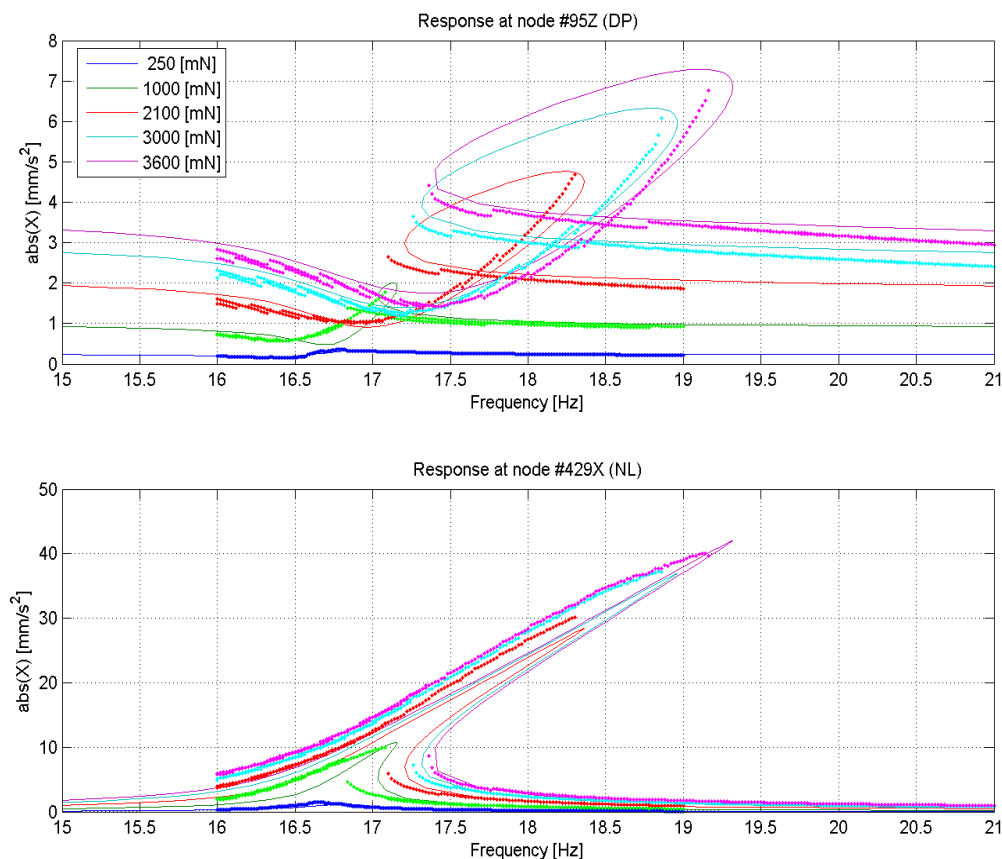


Figure 16 – Acceleration levels for driving point (top) and pylon point (bottom) across several force levels, after updating.

#### 4.5 Validation and Design Modifications

The final step in model validation is to compare predicted response data from the newly generated nonlinear FE Model against some test data not used in the prior nonlinear identification or model update steps. In this case, we chose to validate against a structural modification which we could accurately control; the main mass of

the Pylon (steel, 0.800 [kg]) was substituted with a piece of aluminium of the same geometry (0.336 [kg]). The same change was made to the nonlinear FE model, by modifying the mass and rotational inertia of the point-element suspended underneath the springs. The results are compared in Figure 17.

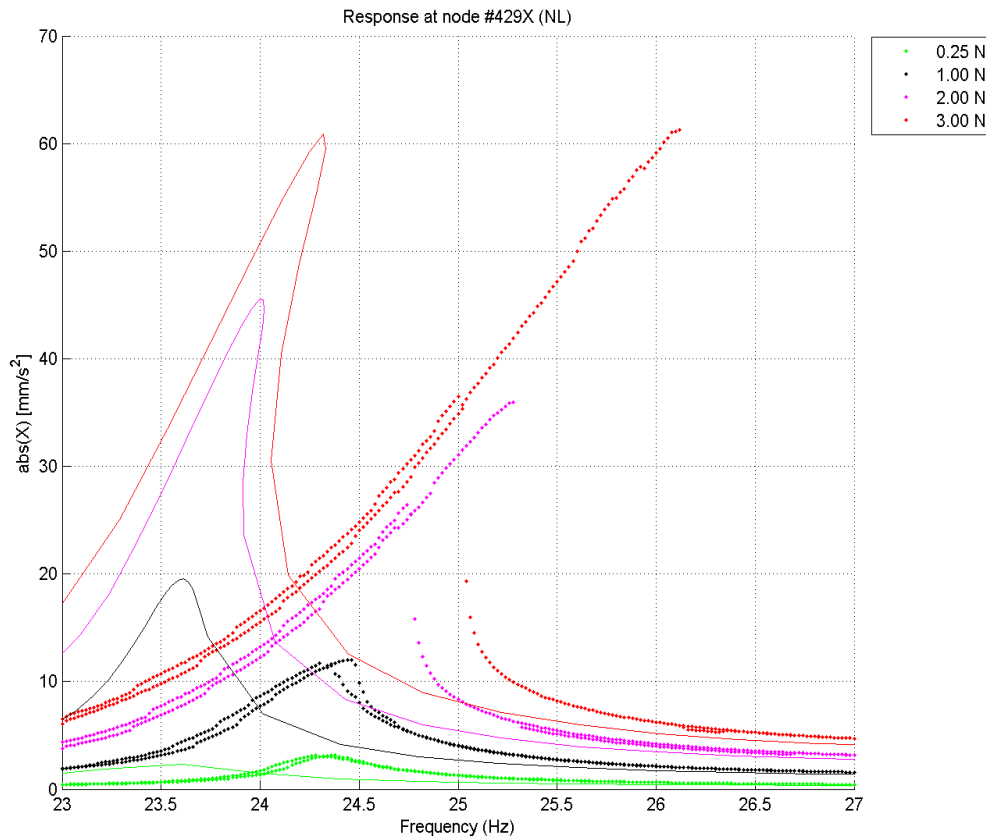


Figure 17 – Acceleration levels of the pylon point after structural modification.

Figure 17 shows that the resonance of the modified model moved from 17.6 [Hz] to 23.5 [Hz], while the actual structure shifted to 24.4 [Hz]. However, this small amount of error was due to the Underlying Linear Model. As one can notice in Table 3, the natural frequencies after the structural modifications are not well-predicted by the Underlying Linear Model, thus making it hard to evaluate the accuracy of the added nonlinear terms. The augmented (upgraded) FE model was observed to preserve the general shape of the response curves caused by the nonlinearities.

This example is indicative of the requirement for a better definition of the errors coming from the ULM and the ones coming from the NL terms. Here, the error in the ULM was quantified by looking at the relative errors of predicted natural frequencies and mode shapes. While the frequency shifts will affect the horizontal position of the backbone curve (i.e. the position of the peak value) the mode shape values (in the form of MAC) dictate how much the degrees of freedom are moving relative to each other, and this will affect greatly the 'shape' of the response curve, making it more or less nonlinear.

The error due to the NL elements can be quantified by normalising both acceleration responses and using the Frequency Domain Assurance Criterion (FDAC) as an indicator of good correlation. FDAC is a model validation technique discussed in [16] [17] that extends the formula of the Modal Assurance Criterion to encompass Frequency Response Functions (or Acceleration Responses, as in our case). It is particularly useful in this case, since it is insensitive to the relative scale factor of two responses and to the frequency shift that might affect them. In addition, it does not require that the responses be defined at the same frequency points, making it a very good tool for the correlation of the 'shape' of the responses.

Mode Pair	STEEL			ALU		
	frequency discrepancy [%]	MAC [%]	FDAC [%]	frequency discrepancy [%]	MAC [%]	FDAC [%]
2	0.21	94.6	96.1	-3.69	68.8	92.5
3	4.10	96.7	97.3	2.82	67.1	88.1

*Table 3 - Error-breakdown for linear model (frequency/MAC) and nonlinear elements (FDAC) for both the steel and aluminium pylon (highest force level, pylon point).*

Table 3 shows how the error is distributed among ULM and NL terms for both the steel and aluminium pylon cases.

For the steel pylon, the frequency discrepancies are low and MAC values are high. This indicates that the ULM is a good descriptor of the responses at the lower energies, and the FDAC values show that the shape of the response curves is generally preserved for each mode.

For the aluminium case, the Underlying Linear Model (modified only to the extent to reflect the changes to the mass and rotary inertia of the new pylon) fails to predict the resonance frequencies of the new structure, and this is reflected in a frequency shift between the simulated and experimental response curves and overall lower values of the MAC. This lower MAC in turn affects the FDAC and the overall shape of the response curves, resulting in a slightly lower nonlinear effect perceived by the structure.

This behaviour can easily be corrected by re-updating the ULM to match the modal parameters of the new structure with the aluminium pylon, but this goes beyond the scope of this section, which is to assess whether and to which extent a nonlinear model is robust with respect to design modifications.

It is important to notice though that this kind error breakdown is only valid if the modifications do not affect the previously identified nonlinear elements (e.g. structural changes to the joints). If such modifications were made, then the new nonlinear structure must be identified again, with some benefits coming from the increased operator knowledge regarding the previous NL system.

In conclusion, in order to make predictions based on previously identified NL elements it is paramount that the ULM is robust enough to produce accurate results over a range of structural/geometrical modifications.

Discussing the validity of the nonlinear model, it is worth mentioning that if some confidence can be put into the prediction of responses to force levels that lie inside the force-range used for identification, the same is not true for force levels that lie outside this range. Extrapolation might lead to poor results, especially if the nonlinear elements are modelled using functionals that suffer from instability phenomena at the boundaries like polynomials. It is then advisable to perform at least one test to the highest possible level representative of a real operational condition or use a different basis for the construction of the functionals (e.g. splines) in order to avoid these kind of issues and retrieve much more reliable characteristics for the nonlinear elements.

Once the nonlinear elements have been included in the equations of motion and the nonlinear model validated, it is possible to perform other nonlinear analyses in order to encompass the presence of rich dynamics, instability phenomena, bifurcations and chaos. In addition, the recovered nonlinear elements can be added in the FE model software in form of discrete springs and dashpots that obey the given functionals and thus be used for special time-marching analyses like stress calculation under coupled thermal/mechanical loads.

#### **4.6 Summary of Phase III**

Phase III comprised the steps of model upgrading, model updating and model validation.

Model upgrading has been introduced as an additional step in the whole validation procedure, and it is necessary in order to augment the linear model and extend its capabilities into the nonlinear range. Model upgrading has been performed by means of implementation of the nonlinear terms in the equations of motion resulting from mass and stiffness matrices of an appropriately-defined preliminary model.

Model updating is nothing more than the standard optimisation procedure to deal the right numerical values of all the new parameters now in the model. It was achieved by means of a widely used and standard MATLAB unconstrained optimisation routine based on the Nelder-Mead simplex direct search.

Model validation is the process of assessing whether the retrieved nonlinear model is capable to describe the dynamics of the nonlinear system under investigation. This has been explored by making physical design modifications to the structure (changing the pylon from steel to aluminium) and assessing whether the nonlinear model was robust enough to predict the change in the responses. It was found that while the general 'shape' of the response curves was preserved, an exact match was not achieved due to deficiencies in the underlying linear model, as evidenced by the inaccuracy of the mode shapes.

## 5 Conclusions and future work

This article provides a first demonstration of a newly introduced procedure for the extension of the existing modal testing technologies to encompass nonlinear dynamical systems.

The overall objectives were (i) to outline a pragmatic approach to the modal testing of nonlinear structures (ii) address the identification of the nonlinear elements that act over the Underlying Linear Model (iii) Augment (*Upgrade*) and correct (*Update*) the ULM, accommodating those elements and (iv) check the validity of the upgraded model across structural modifications.

The approach was laid out in both a concept-driven (Figure 1) and data-driven (Figure 2) 3-phase paradigm (Section 1). Tests were performed (Section 2) and all the properties of the nonlinear elements have then been identified using a mixture of nonlinear methods, static tests and operator knowledge (Section 3). These were finally embedded in the ULM (*Upgrading*) and updated in order to match the measured responses (Section 4). The robustness of the nonlinear model was then checked across a simple structural modification, leading to the error-breakdown analysis and the conclusion that most of the discrepancies might be attributed to inaccuracies of the ULM. Specifically, poor MAC values (inaccuracies regarding the mode shapes) have an important effect on the nonlinearities, since the relative displacement of the degrees of freedom involved in the nonlinear elements is altered as a function of excitation level. These issues, however, might be overcome by re-updating the ULM.

On future grounds, being this approach not fully established yet, there is a broad range of aspects which one could improve upon. Most of these regard phases II and III, since phase I is mostly based on the fully established modal testing procedures.

Phase II consists of the four modules of detection, characterisation, location and quantification that are needed to thoroughly define the nonlinear elements. As it stands now, there are not many methods that can provide these analyses, and the ones that can actually do it, usually suffer from a range of difficulties that can only be overcome with a good knowledge of the structure under investigation (i.e. skilled operator). There is the need to develop more algorithms and methods capable to address the main features of the nonlinear elements in physical space.

Phase III is probably the phase that will benefit the most from future research on the validation of nonlinear models, which is still a rather unexplored field. First of all, the simulation of nonlinear systems in frequency domain is generally conducted using harmonic balance techniques under continuation. This is usually a truncation of the exact solution, and might be not good enough for cases of harsh nonlinearity like

backlash. Especially important is also the ability to discern the errors that arise from poor nonlinear elements from errors that come from a sub-par underlying linear model. In our case, the frequency shifts and MAC values were used as indicators of the goodness of the ULM, while the Frequency Domain Assurance Criterion was used as a metric to assess that the overall shape of the response curves was preserved.

## 6 Acknowledgements

The authors want to acknowledge the support of the 'Engineering Nonlinearity' program (funded by EPSRC, Grant Reference EP/K003836/2) for providing the test structure.

## 7 References

- [1] D. Ewins, B. Weekes and A. delli Carri, "Modal Testing for Model Validation of Structures with Discrete Nonlinearities," *Philosophical Transactions A*, 2015.
- [2] A. Josefsson, M. Magnevall and K. Ahlin, "Control Algorithm For Sine Excitation On Nonlinear Systems," *IMAC XXIV Conference, Society for Experimental Mechanics*, 2006.
- [3] B. Weekes and D. Ewins, "Multi-frequency, 3D ODS measurement by continuous scan laser Doppler vibrometry," *Mechanical Systems and Signal Processing*, Vols. 58-59, p. 325–339, 2015.
- [4] J. Bendat, P. Palo and R. Coppolino, "A general identification technique for nonlinear differential equations of motion," *Probabilistic Engineering Mechanics*, vol. 7, no. 1, pp. 43-61, 1992.
- [5] G. Kerschen, V. Lenaerts and J. Golinval, "Identification of a continuous structure with a geometrical non-linearity, part 1: conditioned reverse path method," *Journal of Sound & Vibration*, vol. 262, pp. 889-906, 2003.
- [6] S. Marchesiello, "Application of the Conditioned Reverse Path Method," *Mechanical Systems and Signal Processing*, vol. 17, no. 1, pp. 183-188, 2003.
- [7] C. Richards and R. Singh, "Identification of Multi-Degree-of-Freedom Non-Linear Systems Under Random Excitations by the "Reverse Path" Spectral Method," *Journal of Sound and Vibration*, vol. 213, no. 4, pp. 673-708, 1998.

- [8] C. Runge, "Über empirische Funktionen und die Interpolation zwischen äquidistanten Ordinaten," *Zeitschrift für Mathematik und Physik*, vol. 46, p. 224–243, 1901.
- [9] J.-P. Noel, *A Frequency-domain Approach to Subspace Identification of Nonlinear Systems*, University of Liege, 2014.
- [10] J. A. Nelder and R. Mead, "A Simplex Method for Function Minimization," *The Computer Journal*, vol. 7, no. 4, pp. 308-313, 1965.
- [11] M. Platten, J. Wright, J. Cooper and G. Dimitriadis, "Identification of a Nonlinear Wing Structure Using an Extended Modal Model," *Journal of Aircraft*, vol. 46, no. 5, pp. 1614-1626, 2009.
- [12] M. Paz, "Dynamic Condensation," *AIAA Journal*, vol. 22, no. 5, pp. 724-727, 1984.
- [13] J. O'Callahan, P. Avitabile and R. Riemer, "System Equivalent Reduction Expansion Process," *Seventh International Modal Analysis Conference*, 1989.
- [14] Y. Cheung, S. Chen and S. Lau, "Application of the incremental harmonic balance method to cubic non-linearity systems," *Journal of Sound and Vibration*, vol. 140, no. 2, pp. 273-286, 1990.
- [15] E. Petrov and D. Ewins, "State-of-the-art dynamic analysis for non-linear gas turbine structures," *Proceedings of the Institution of Mechanical Engineers, Part G: Journal of Aerospace Engineering*, vol. 218, no. 3, pp. 199-211, 2004.
- [16] R. Pascual, J. Golinval and M. Razeto, "A frequency domain correlation technique for model correlation and updating," *Proceedings of the 15th International Modal Analysis Conference*, pp. 587-592, 1997.
- [17] W. Heylen and S. Lammens, "FRAC: A Consistent way of Comparing Frequency Response Functions," in *International Conference on Identification in Engineering*, Swansea, 1996.

## **8 Appendix: Reverse Path method for characterisation and location of nonlinearities**

The Reverse Path method was initially proposed by Bendat in 1990 and later refined in 1992 [4]. The method is known as "reverse path" since the input and output quantities are reversed (Figure 19). The processing is performed in the frequency domain using conventional Multiple-Input-Single-Output (MISO) techniques and

estimates of both the Underlying Linear Model and the nonlinearity locations and types are obtained from a single analysis.

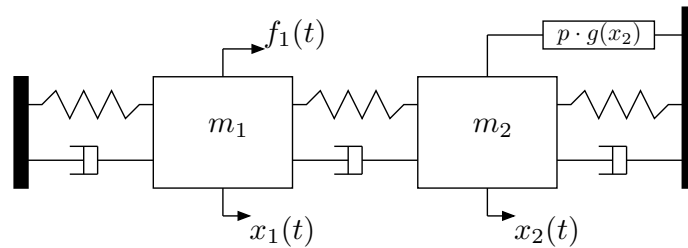


Figure 18 – A system with grounded nonlinearity described by a nonlinear operator  $g(\cdot)$  and coefficient  $p$

In order to explain the reverse path technique, the simple 2DOF system presented in Figure 18 is used. This system can be modeled in the frequency domain as

$$\begin{Bmatrix} X_1 \\ X_2 \end{Bmatrix} = \begin{bmatrix} H_{11} & H_{12} \\ H_{21} & H_{22} \end{bmatrix} \begin{Bmatrix} F_1 \\ -P \cdot \mathcal{F}(g(x_2)) \end{Bmatrix}$$

The matrix formulation can thus be expanded in the equations

$$X_1 \cdot H_{11}^{-1} + \frac{H_{12}}{H_{11}} \cdot P \cdot \mathcal{F}(g(x_2)) = F_1$$

$$X_2 \cdot H_{21}^{-1} + \frac{H_{22}}{H_{21}} \cdot P \cdot \mathcal{F}(g(x_2)) = F_1$$

Each of these equations can be rearranged in a reverse-path fashion with the forces at the output, actually forming a set of MISO analyses, one per DOF (Figure 19).

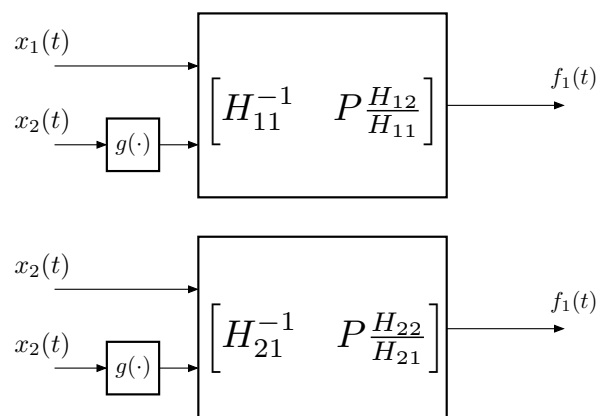


Figure 19 - The 2DOF system is broken into two MISO analyses

The inputs of the MISO analyses consist of a single measured DOF and all the nonlinearities present in the system. If the location or the type of nonlinearity is unknown, one can feed guesses into the system and use the multiple coherence function as an index for the goodness of estimation.



$$\gamma^2 = \frac{G_{FX}G_{XX}^{-1}G_{FX}^H}{G_{FF}}$$

Where  $G$  represents the cross-spectra matrices between inputs  $F$  and outputs  $X$ .

The multiple coherence function is a linear relationship that measures the causality between one output and all the input signals. As the standard coherence, it ranges between 0 (no correlation) and 1 (the output is completely caused by the input). The coherence function for a nonlinear system will always be less than unity because of the linear nature of the coherence operator.

As long as the guesses are good enough, the multiple coherence function will continue to improve over the frequency range and eventually it will be maximised when all the nonlinearities have been characterised and localised.

The guessing process can be totally blindfolded, iterating over previously defined locations and nonlinear characteristics, but it also permits the user to exploit any knowledge of where or what type of nonlinearity might be present. Once the best coherence has been achieved, the selected guesses can be used to quantify their coefficients.

The Reverse Path method needs time histories of forces, displacements and velocities acquired using a broadband excitation. Time histories are needed because they have to pass through the nonlinear operator before they get transformed into the frequency domain and fed to the system. Displacements are used to construct stiffness-based nonlinearities and velocities are used to construct damping-based ones. To retrieve displacements and velocities one could generally integrate the accelerations with appropriate filtering; this reduces the accuracy of the quantification using the reverse path method, but does not affect the location and characterisation steps.